Immunohistochemical double nuclear staining for cell-specific automated quantification of the proliferation index - A promising diagnostic aid for melanocytic lesions

Brogård, Mette Bak; Nielsen, Patricia Switten; Christensen, Kristina Bang; Georgsen, Jeanette Bæhr; Wandler, Anne; Lade-Keller, Johanne; Steiniche, Torben

Published in:
Pathology - Research and Practice

DOI (link to publication from Publisher):
10.1016/j.prp.2024.155177

Publication date:
2024

Document Version
Publisher's PDF, also known as Version of record

Pathology - Research and Practice 255 (2024) 155177

Contents lists available at ScienceDirect

Pathology - Research and Practice

journal homepage: www.elsevier.com/locate/prp

Immunohistochemical double nuclear staining for cell-specific automated quantification of the proliferation index – A promising diagnostic aid for melanocytic lesions

Mette Bak Brogård [a,b,*], Patricia Switten Nielsen [a,b], Kristina Bang Christensen [a], Jeanette Bæhr Georgsen [a,b], Anne Wandler [a], Johanne Lade-Keller [c], Torben Steiniche [a,b]

[a] Department of Pathology, Aarhus University Hospital, Palle Juul-Jensens Boulevard 35, 8200 Aarhus N, Denmark
[b] Department of Clinical Medicine, Aarhus University, Palle Juul-Jensens Boulevard 99, 8200 Aarhus N, Denmark
[c] Department of Pathology, Aalborg University Hospital, Ladegårdsgade 3, 9000 Aalborg, Denmark

ARTICLE INFO

Keywords:
Melanocytic lesions
Proliferation index
Ki67
Multiplex immunohistochemistry
Digital pathology
Digital image analysis

ABSTRACT

Aims: Pathologists often use immunohistochemical staining of the proliferation marker Ki67 in their diagnostic assessment of melanocytic lesions. However, the interpretation of Ki67 can be challenging. We propose a new workflow to improve the diagnostic utility of the Ki67-index. In this workflow, Ki67 is combined with the melanocytic tumour-cell marker SOX10 in a Ki67/SOX10 double nuclear stain. The Ki67-index is then quantified automatically using digital image analysis (DIA). The aim of this study was to optimise and test three different multiplexing methods for Ki67/SOX10 double nuclear staining.
Methods: Multiplex immunofluorescence (mIF), multiplex immunohistochemistry (mIHC), and multiplexed immunohistochemical consecutive staining on single slide (MICSSS) were optimised for Ki67/SOX10 double nuclear staining. DIA applications were designed for automated quantification of the Ki67-index. The methods were tested on a pilot case-control cohort of benign and malignant melanocytic lesions (n = 23).
Results: Using the Ki67/SOX10 double nuclear stain, malignant melanocytic lesions could be completely distinguished from benign lesions by the Ki67-index. The Ki67-index cut-offs were 1.8% (mIF) and 1.5% (mIHC and MICSSS). The AUC of the automatically quantified Ki67-index based on double nuclear staining was 1.0 (95% CI: 1.0;1.0), whereas the AUC of conventional Ki67 single-stains was 0.87 (95% CI: 0.71;1.00).
Conclusions: The novel Ki67/SOX10 double nuclear stain highly improved the diagnostic precision of Ki67 interpretation. Both mIHC and mIF were useful methods for Ki67/SOX10 double nuclear staining, whereas the MICSSS method had challenges in the current setting. The Ki67/SOX10 double nuclear stain shows potential as a valuable diagnostic aid for melanocytic lesions.

1. Introduction

The assessment of melanocytic lesions can be challenging even for experienced dermatopathologist, with a high risk of misclassification [4,8]. Since there is no single histologic feature that is pathognomic to melanomas, the diagnosis is based on an interpretation of several features, of which many can be observed in benign nevi as well [13]. Therefore, dermatopathologists commonly use immunohistochemistry (IHC) to assist their evaluation.

One of the most commonly used IHC markers is the nuclear proliferation marker Ki67 since malignant lesions in general exhibit a higher Ki67-index than benign lesions [7]. However, there are two key challenges to the diagnostic utility of the Ki67-index. First, manual precision counting using a microscope is laborious and time-consuming, why in practise, pathologists often turn to eyeballing, leading to poor accuracy and low reproducibility [22]. Second, Ki67 positivity is not limited to melanocytic cells; thus, other proliferative cells may be misinterpreted, for example, infiltrating lymphocytes, as proliferative melanocytes [7]. This insufficient tumour-cell identification may lead to overestimation of the proliferation index, especially in inflamed lesions.

To solve the first problem, there has been a growing interest in developing digital image analysis (DIA) algorithms for automated

* Corresponding author at: Department of Pathology, Aarhus University Hospital, Palle Juul-Jensens Boulevard 35, 8200 Aarhus N, Denmark.
E-mail addresses: mettbrog@clin.au.dk, mettbrog@rm.dk (M.B. Brogård).

https://doi.org/10.1016/j.prp.2024.155177
Received 20 November 2023; Received in revised form 10 January 2024; Accepted 26 January 2024
Available online 1 February 2024

quantification of the Ki67-index [9,14,16]. However, the diagnostic utility of DIA has been challenged by the second problem, the insufficient tumour-cell identification, since the algorithms need to know which cells to count as tumour cells. Consequently, a tumour-cell marker is required. Our research group has previously used MART1 as a melanocytic tumour-cell marker and has shown that the Ki67/MART1 double stain results in a good diagnostic performance, both with manual and DIA quantification [17–19, 32]. The Ki67/MART1 double stain is now frequently used for manual assessment of Ki67 in melanocytic lesions.

The Ki67/MART1 double stain still has two major limitations. First, MART1 is a cytoplasmic stain and Ki67-positive lymphocytes in the tumour area can still be incorrectly interpreted when overlying the MART1-positive melanocytic cytoplasm [17]. Second, MART1 is absent in 8–25% of melanomas, unfortunately often challenging lesions as spindle and desmoplastic melanomas [13,20]. Hence, we propose a Ki67/SOX10 double nuclear staining to further improve the assessment of the Ki67-index in melanocytic lesions. SOX10 is a marker with a high sensitivity for melanocytes, also in the MART1 negative lesions [27,29]. Furthermore, SOX10 is a nuclear marker, like KI67, and the use of two nuclear markers ensures accurate identification owing to their co-localisation. Indeed, the combination of a target biomarker with a tumour-cell marker in a double nuclear stain can serve as an optimal platform for quantitative digital image analysis in cancer tissue.

Co-localised staining is challenging with conventional IHC since the two markers obscure each other, but newer staining techniques may be utilised [30]: a) Multiplex immunofluorescence (mIF), that is used in research for co-localised biomarkers [2,10,34], b) Multiplex immunohistochemistry (mIHC), where certain combinations of chromogens can yield a colour shift when co-localised [6,31], and c) Multiplexed immunohistochemical consecutive staining on single slide (MICSSS), where mono-IHC stains are performed in consecutive cycles of stain, scan, and de-staining [1,23].

The aim of this study was to: a) describe and optimise three different methods for Ki67/SOX10 double nuclear staining to enhance the diagnostic utility of automatically quantified Ki67-indexes in melanocytic lesions; b) test the methods' ability to distinguish between benign and malignant melanocytic lesions, when incorporated into a workflow with DIA. To our knowledge, this is the first study that uses double nuclear staining for automated quantification of the Ki67-index in melanocytic lesions.

2. Methods

2.1. Material

The retrospective cohort of primary cutaneous melanocytic lesions for this case-control study comprised 10 superficial spreading melanomas (SSM), 10 compound nevi (CN) diagnosed at Aarhus University Hospital (AUH), Denmark from Marts 2018 to June 2018. The SSM were matched with CN based on tumour thickness and requisition date. We wanted to match SSM and CN because they both have dermo-epidermal activity and share several morphological features that can make the distinction difficult. We focussed on the Union for International Cancer Control (UICC) TNM-stage T1b melanomas since thin lesions often are more diagnostically challenging than thick lesions [4,8]. Moreover, sentinel lymph node biopsy is recommended for T1b melanomas, underlining the importance of correct classification of these lesions [11]. In addition, we included three inflamed halo nevi (HN), diagnosed at AUH, Denmark from 2012 to 2020, to challenge the differentiation between proliferating tumour cells and proliferating lymphocytes. Formalin-fixed and paraffin-embedded (FFPE) tissue blocks were retrieved from the archive at the Department of Pathology, Aarhus University Hospital, Denmark.

Ethical approval for this study was waived by the Regional Committees on Health Research Ethics and the Central Denmark Region, who considered it a method study.

2.2. Multiplex immunofluorescence (mIF)

A mIF staining protocol was optimized for double nuclear staining with steps as described in Fig. 1A-B. mIF stains were performed on Ventana Discovery Ultra (Ventana Medical Systems, Inc., Tuscon, Arizona USA) using standard settings and reagent kits. First, 2–3 μm slides were incubated with primary SOX10-antibody (monoclonal rabbit, clone SP267, ready-to-use, Ventana) for 60 min, followed by secondary anti-rabbit antibody (DISCOVERY omniMap anti-Rb HRP, Ventana) and DCC fluorophore (DISCOVERY DCC kit, Ventana). Then, the first set of antibodies were denatured in a citrate-based buffer, pH 6.5 (RiboCC Solution, CC2, Ventana) for 8 min at 100 °C. Next, slides were incubated with primary Ki67-antibody (monoclonal rabbit, clone 30–9, ready-to-use, Ventana) for 60 min followed by secondary anti-rabbit antibody (DISCOVERY ultraMap anti-Rb HRP, Ventana) and Cy5 fluorophore (DISCOVERY Cy5 kit, Ventana), dehydrated and mounted with antifade mounting medium with DAPI (VECTASHIELD®, Vector Laboratories, Inc., Burlingame, USA). Whole slide images of the mIF stains were captured at 40X magnification using Nanozoomer QS60 (Hamamatsu Photonics K.K., Hamamatsu City, Japan) with fixed fluorescens exposure settings (Fig. 1A, step1). The fluorescence filters used was DAPI (focus filter), DCC, and Cy5. Then, the cover glasses were removed by heat, and the slides re-stained with haematoxylin and eosin (HE) in routine settings and re-scanned (Fig. 1A, step 2).

2.3. Multiplex chromogenic immunohistochemistry (mIHC)

A mIHC protocol was optimized for double nuclear staining with steps as described in Fig. 1C-D. First, 2–3 μm slides were stained with HE in routine settings and scanned (Fig. 1C, step 1). Then, the cover glasses were removed by heat (90 °C), and the slides were re-stained with mIHC performed on Ventana Discovery Ultra (Ventana Medical Systems, Inc., Tuscon, Arizona USA) using standard settings and reagent kits (Fig. 1C, step 2): The slides were incubated with primary SOX10-antibody (monoclonal rabbit, clone SP267, ready-to-use, Ventana) for 60 min, followed by secondary anti-rabbit antibody (DISCOVERY ultraMap anti-Rb HRP, Ventana) and purple chromogen (DISCOVERY Purple kit, Ventana). Then, the first set of antibodies were denatured at 100 °C for 8 min in citrate-based buffer, pH 6.5 (RiboCC Solution, CC2, Ventana). Next, slides were incubated with primary Ki67-antibody (monoclonal rabbit, clone 30–9, ready-to-use, Ventana) for 32 min followed by secondary anti-rabbit antibody (DISCOVERY ultraMap anti-Rb HRP, Ventana) and Teal chromogen (DISCOVERY Teal HRP kit, Ventana). The slides were not counterstained. Finally, whole slide images of mIHC stains were captured in brightfield at 40X magnification using Nanozoomer 2.0 HT (Hamamatsu Photonics K.K., Hamamatsu City, Japan).

2.4. Multiplexed immunohistochemical consecutive staining on single slide (MICSSS)

A MICSSS protocol was optimized for double nuclear staining with steps as described in Fig. 1E-F. MICSSS was performed on BenchMark Ultra (Ventana Medical Systems, Inc., Tuscon, Arizona USA) using standard settings and reagent kits. First, 2–3 μm slides were incubated with primary Ki67-antibody (monoclonal rabbit, clone 30–9, ready-to-use, Ventana) for 32 min, visualized by Fast Red (UltraView Alkaline Phosphatase Red Detection Kit, Ventana), counterstained with Mayer's haematoxylin, dehydrated and mounted with xylen. Whole slide images of first stain were captured at 40X magnification using Nanozoomer 2.0 HT (Hamamatsu Photonics K.K., Hamamatsu City, Japan) (Fig. 1E, step 1). Then, the cover glasses were removed by acetone and xylen and slides washed in alcohol baths for a total of 125 min to remove the Fast Red stain. Then, incubated in citrate-based buffer, pH 6.5 (RiboCC Solution, CC2, Ventana) to denature first set of antibodies. Next, slides were incubated with primary SOX10-antibody (monoclonal rabbit, clone SP267, ready-to-use, Ventana) for 32 min, visualized by DAB

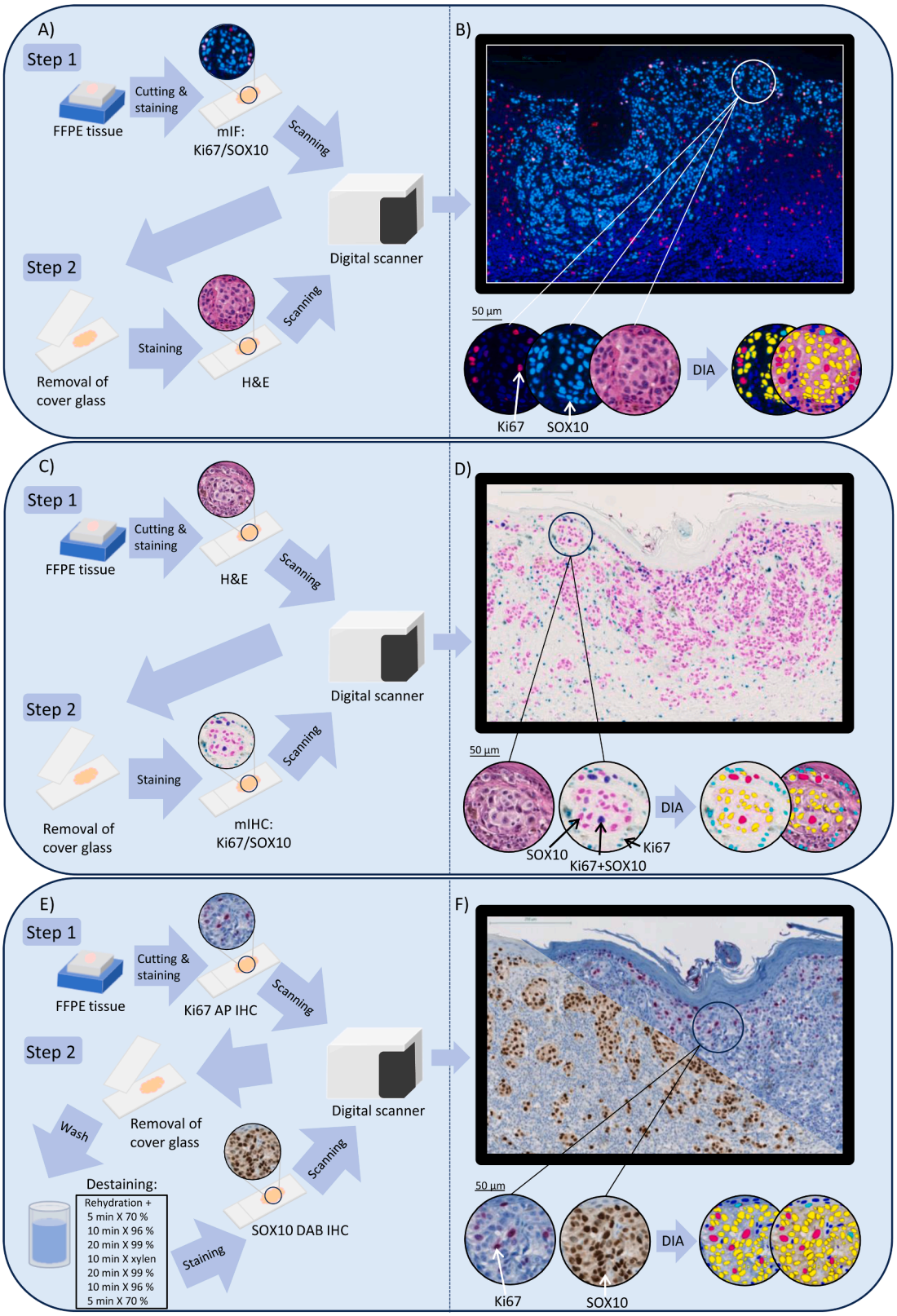

Fig. 1. Schematic presentation of staining procedures and resulting images of double nuclear staining with three different methods. A) Multiplex immunofluorescence (mIF). One tissue section was stained with Ki67/SOX10 mIF and scanned (Step 1). Then the cover glass was removed, and the same slide stained with HE and scanned (Step 2). C) Multiplex chromogenic immunohistochemistry (mIHC). One tissue section was stained with HE and scanned (Step 1). Then the cover glass was removed, and the same slide was stained with Ki67/SOX10 mIHC and scanned (Step 2). E) Multiplexed immunohistochemical consecutive staining on single slide (MICSSS). One tissue section was stained with Ki67 Fast Red and scanned (Step 1). Then the cover glass was removed, and the slide was destained, before second staining with SOX10 DAB and scanning (Step 2). B, D, & F) Examples of resulting images from the same case of malignant melanoma, stained with either mIF (B), mIHC (D) or MICSSS (F). The images were aligned digitally and analysed using digital image analysis (DIA). DIA markers: Red: Ki67-positive melanocyte. Yellow: Ki67-negative melanocyte. Light blue: Ki67-positive non-melanocytic cell. Dark blue: Ki67-negative non-melanocytic cell.

(OptiView DAP IHC Detection Kit, Ventana), counterstained with Mayer's haematoxylin and bluing agent, dehydrated, mounted and re-scanned (Fig. 1E, step 2).

2.5. Digital image analysis

DIA was performed using Visiopharm Integrator System 2020.08.2.8800 (Visiopharm A/S, Hoersholm, Denmark), and comprised image alignment, region outlining, nuclei identification and classification and, finally, index quantification. The digital scans of stains performed on the same tissue section were aligned automatically using Visiopharm's Tissuealign™. An experienced dermato-pathologist (TS) roughly outlined a region of interest (ROI) containing the melanocytic lesion including both the epidermal and dermal compartment on the digital HE slides. To compare the methods, the tumour ROI outlined on digital HE of the mIHC method was copied to the digital slides of the other methods. The border between epidermis and dermis was outlined manually to divide the tumour ROI in these two compartments.

The nuclei were identified using Visiopharm's pre-trained Deep Learning (U-net) application. The application was retrained on manually labelled nuclei in a few colour-representative cases to fit each of the staining methods. Postprocessing steps were added to each application using fixed thresholds to classify the identified nuclei according to Ki67 and SOX10 positivity. The mIF-thresholds were based on the fluorescence intensity of the DCC (SOX10, blue) and Cy5 (Ki67, red) filters, and the mIHC and MICSSS thresholds were based on RGB colour bands filters. The thresholds were established through close comparison with the chromogenic controls for Ki67 and SOX10, performed as routine stains.

2.6. Quantitative analyses

The Ki67-index was quantified automatically by Visiopharm applications on basis of the annotated nuclei in the outlined ROIs. We quantified the Ki67-indexes of both the dermal ROI, the epidermal ROI, and the total tumour ROI, as well as the whole tissue ROI. The Ki67-index was defined as the number of Ki67-positive melanocytic cells divided by the total number of melanocytic cells:

$$Ki67index = \frac{N_{Ki67^+SOX10^+}}{N_{SOX10^+} + N_{Ki67^+SOX10^+}} \bullet 100\%$$

2.7. Statistical analyses

Data analysis was performed in STATA 17.0 (StataCorp, College Station, TX, USA). Benign (CN and HN) and malignant (SSM) lesions were compared by Wilcoxon rank sum Mann-Whitney tests (median Ki67-indices, tumour ROI area and number of melanocytes), exact t-test (patient ages), Fishers exact test (gender), or Spearmans rank correlation (location). A two-sided P value < 0.05 was considered statistically significant. The diagnostic performance was evaluated by area under curve (AUC) of Receiver Operating Characteristics (ROC). Sensitivity and specificity were calculated by Ki67-index cut-offs defined as the level just below the lowest malignant lesion.

3. Results

3.1. Cohort characterisation

Patient and tumour characteristics are listed in Table 1. Benign and malignant cases did not differ significantly in relation to tumour thickness, tumour location, or sex. However, they differed in patient age ($P = 0.002$). There was no statistically significant difference in the median tumour area (ROI) ($P = 0.172$) or in the mean number of melanocytes ($P = 0.083$) between benign and malignant melanocytic lesions in this cohort.

Table 1
Patient and tumour characteristics

Feature	Malignant (n: 10)	Benign (n: 13)
Age in years, mean (SD)	63.7 (13.5)	42.6 (14.0)
Sex		
Female, no. (%)	4 (40)	6 (46)
Male, no. (%)	6 (60)	7 (54)
Location		
Head, no. (%)	0 (0)	1 (8)
Trunk, no. (%)	3 (30)	3 (23)
Back, no. (%)	3 (30)	2 (15)
Upper limb, no. (%)	2 (20)	4 (31)
Lower limb, no. (%)	2 (20)	2 (15)
Unknown, no. (%)	0 (0)	1 (8)
Thickness[a] in mm, mean (SD)	0.93 (0.12)	0.92 (0.21)
Ulceration, no. (%)	1 (10)	0 (0)

[a] Thickness measured as Breslow thickness for superficial spreading melanoma and likewise for compound nevi and halo nevi.

3.2. Double nuclear staining methods

The optimised mIF staining protocol resulted in clear florescent images with an easy separation of the two markers by fluorescence filters (Fig. 1B). The double nuclear staining with the mIHC method resulted in bright staining of SOX10 or Ki67 mono-positive nuclei and a distinct colour change to dark blue in the double positive nuclei, demonstrated in Fig. 1D. By aligning the mIF and mIHC stains with the HE stains performed on the same tissue slides, we achieved a clear visualization of tissue morphology. The MICSSS staining is demonstrated in Fig. 1F where the two mono stains preformed on the same tissue slide are aligned, resulting in a virtual double nuclear stain.

All mIF stains succeeded when stained with the final protocol. However, in one case, an area of autofluorescence was manually removed before conducting the DIA. Three cases of mIHC stains had to be repeated because of thick slides resulting in overlying nuclei and intensely dark stained nuclei. Despite several attempts of optimisation, the final MICSSS protocol did not result in complete removal of the Fast Red chromogen. Therefore, eight out of 23 cases had to be excluded from the analysis.

3.3. The Ki67-index distinguished between malignant and benign melanocytic lesions

As shown in Table 2, the median of the automatically quantified Ki67-indexes was significantly higher in the malignant melanocytic lesions than the benign. This was evident for Ki67-indexes based on all three staining methods. The malignant melanocytic lesions could be completely distinguished from the benign lesions by a Ki67-index cut-off of 1.8% (mIF stain) or 1.5% (mIHC stain) (Fig. 2). When excluding the eight cases with incomplete de-staining from the MICSSS analysis, a similar cut-off could likewise separate benign and malignant lesions.

3.4. Tissue regions for analysis

The quantification of the Ki67-index was performed automatically on both manually outlined tumour areas including overlaying epidermis and across the entire tissue sections. Simple outlining of the total tumour region including overlaying epidermis resulted in the highest AUC in all three methods, whereas analysing the whole tissue resulted in lower AUC, especially in the mIF and MICSSS methods (Table 2). Dividing the tumour region in an epidermal and dermal compartment did not add to the performance of the Ki67-index in this cohort.

3.5. Tumour-cell identification enhanced diagnostic performance of the Ki67-index

The diagnostic performance of automatically quantified Ki67-index

Table 2
Results of automated quantification of Ki67-indexes using double nuclear staining and digital image analysis

	Median Ki67-index, BN[a], % (95% CI)	Median Ki67-index, SSM, % (95% CI)	Difference, P value[b]	ROC area, AUC (95% CI)	Ki67-index cut-off, %-point[c]	Mis-classified, n/total	Sensitivity, %	Specificity, %
Multiplex immunofluorescence (mIF) (Total=23, BN=13, SSM=10)								
Total tumour ROI	0.47 (0.20;0.67)	4.34 (2.6;8.96)	< 0.001	1.000 (1.0;1.0)	1.8	0/23	100 (100;100)	100 (100;100)
-Epidermal ROI	2.40 (1.17;2.80)	11.2 (6.35;14.7)	< 0.001	0.985 (0.95;1.0)	3.0	2/23	100 (100;100)	84.6 (69.9;99.4)
-Dermal ROI	0.14 (0.07;0.54)	3.24 (1.33;6.56)	< 0.001	0.977 (0.93;1.0)	0.4	3/23	100 (100;100)	76.9 (59.7;94.1)
Whole tissue ROI	0.59 (0.32;1.56)	3.8 (2.29;9.14)	< 0.001	0.939 (0.85;1.0)	1.5	3/23	100 (100;100)	76.9 (59.7;94.1)
Multiplex chromogenic IHC (mIHC) (Total=23, BN=13, SSM=10)								
Total tumour ROI	0.29 (0.22;0.8)	3.79 (2.58;7.47)	< 0.001	1.000 (1.0;1.0)	1.5	0/23	100 (100;100)	100 (100;100)
-Epidermal ROI	1.14 (0.86;2.07)	10.1 (4.61;15.5)	< 0.001	0.977 (0.93;1.0)	1.8	3/23	100 (100;100)	76.9 (59.7;94.1)
-Dermal ROI	0.22 (0.13;0.47)	2.84 (2.18;5.25)	< 0.001	0.992 (0.97;1.0)	1.0	1/23	100 (100;100)	92.3 (81.4;103)
Whole tissue ROI	0.32 (0.23;0.66)	3.1 (1.71;5.02)	< 0.001	0.985 (0.95;1.0)	1.5	1/23	100 (100;100)	92.3 (81.4;103)
Multiplexed IHC consecutive staining on single slide (MICSSS)[d] (Total=15, BN=9, SSM=6)								
Total tumour ROI	0.17 (0.05;0.86)	5.95 (2.36;14.5)	< 0.001	1.000 (1.0;1.0)	1.5	0/15	100 (100;100)	100 (100;100)
-Epidermal ROI	1.32 (0.55;2.74)	11.0 (4.19;21.6)	0.002	0.963 (0.88;1.0)	3.5	1/15	100 (100;100)	88.9 (72.9;105)
-Dermal ROI	0.10 (0.01;0.46)	5.17 (2.00;8.06)	< 0.001	1.000 (1.0;1.0)	1.5	0/15	100 (100;100)	100 (100;100)
Whole tissue ROI	9.87 (6.13;22.5)	25.5 (13.1;59.1)	0.018	0.870 (0.68; 1.0)	11	4/15	100 (100;100)	55.6 (30.4;80.7)

[a] Abbreviation: BN: Benign nevi; Compound nevi and halo nevi.
[b] Wilcoxon rank sum test (Mann-Withney).
[c] The Ki67-index were chosen to result in no misclassified malignant lesions.
[d] Eight lesions were excluded from MICSSS analysis due to failed stains.

was assessed by ROC-analysis, comparing results with and without verification of tumour cells through double nuclear staining (Fig. 3). The Ki67-index based on the double nuclear staining had an AUC of 1.00 (95% CI: 1.00; 1.00), whereas the Ki67-index based on conventional Ki67 single-stain had an AUC of 0.869 (95% CI: 0.713; 1.00). When the number of Ki67-positive nuclei from the single stain was calculated as a fraction of the tumour area, to closer mimic the clinical 'eyeballing' method, the AUC was 0.800 (95% CI: 0.609; 0.991).

4. Discussion

In this proof-of-concept study, we optimised three immunohistochemical methods for Ki67/SOX10 double nuclear staining. Both mIHC and mIF were useful methods for Ki67/SOX10 double nuclear staining, whereas the MICSSS method had challenges in the current setting as discussed below. Yet, the mIHC method seemed most feasible for routine application (Fig. 4). The novel Ki67/SOX10 double nuclear stain developed in this study correctly classified a test cohort of melanocytic lesions into benign or malignant. Despite the limited cohort size, the findings suggest that the double nuclear stain highly improves the diagnostic precision of Ki67 interpretation, and that automated Ki67 quantification shows potential as an important diagnostic aid. However, the findings must be validated in a larger study cohort.

First, we attempted to perform the Ki67/SOX10 double nuclear stain using conventional chromogen-based immunohistochemistry. However, as reported in the literature [24,31,33], we found that co-localised markers were visually indistinguishable from mono-markers (Fig. S1). Although there has been attempts to separate brown and red chromogens by spectral unmixing, this was only possible with relatively transparent stains [31]. We did not find it possible to separate co-localised red and brown stains with our DIA methods. Therefore, we turned to more experimental multiplex immunohistochemistry.

mIF Ki67/SOX10 staining has the general advantage that it enables concurrent visualisation of multiple markers, even when co-localised [24,34]. mIF utilises various fluorescence filters to differentiate each stain, which makes it optimal for DIA. An important limitation of mIF is the lack of visualization of tissue morphology. To overcome this, we combined the mIF stain with a HE stain performed on the same slide, ensuring optimal visualization of morphology [10,33]. However, mIF gave us additional challenges: 1) difficulties in achieving uniform fluorescence staining intensities across all samples requiring fine-tuning of exposure settings for each scan, 2) fading fluorescent stains (photobleaching), demanding prompt scanning [21,28], 3) tissue autofluorescence, requiring manual correction during image analysis [21, 30], and 4) slow image requisition [2,28,30,33]. These disadvantages can be problematic in a routine workflow.

Therefore, we assessed chromogen-based immunohistochemistry for double nuclear staining, given their stability and fast, standardised scanning.

mIHC Ki67/SOX10 staining can be performed in a single staining procedure using a previously HE-stained slide, causing no additional delay in the diagnostic workflow in a fully digitalised pathology department (Fig. 4). Furthermore, the pathologist can evaluate the mIHC Ki67/SOX10 using conventional light microscopy. Unlike mIF, the mIHC double nuclear stain cannot be isolated into single stains. Instead, a shift in colour is used to identify double positive nuclei, which requires a clear contrast between single and double stained nuclei. We tested several combinations of chromogens and chose a combination of

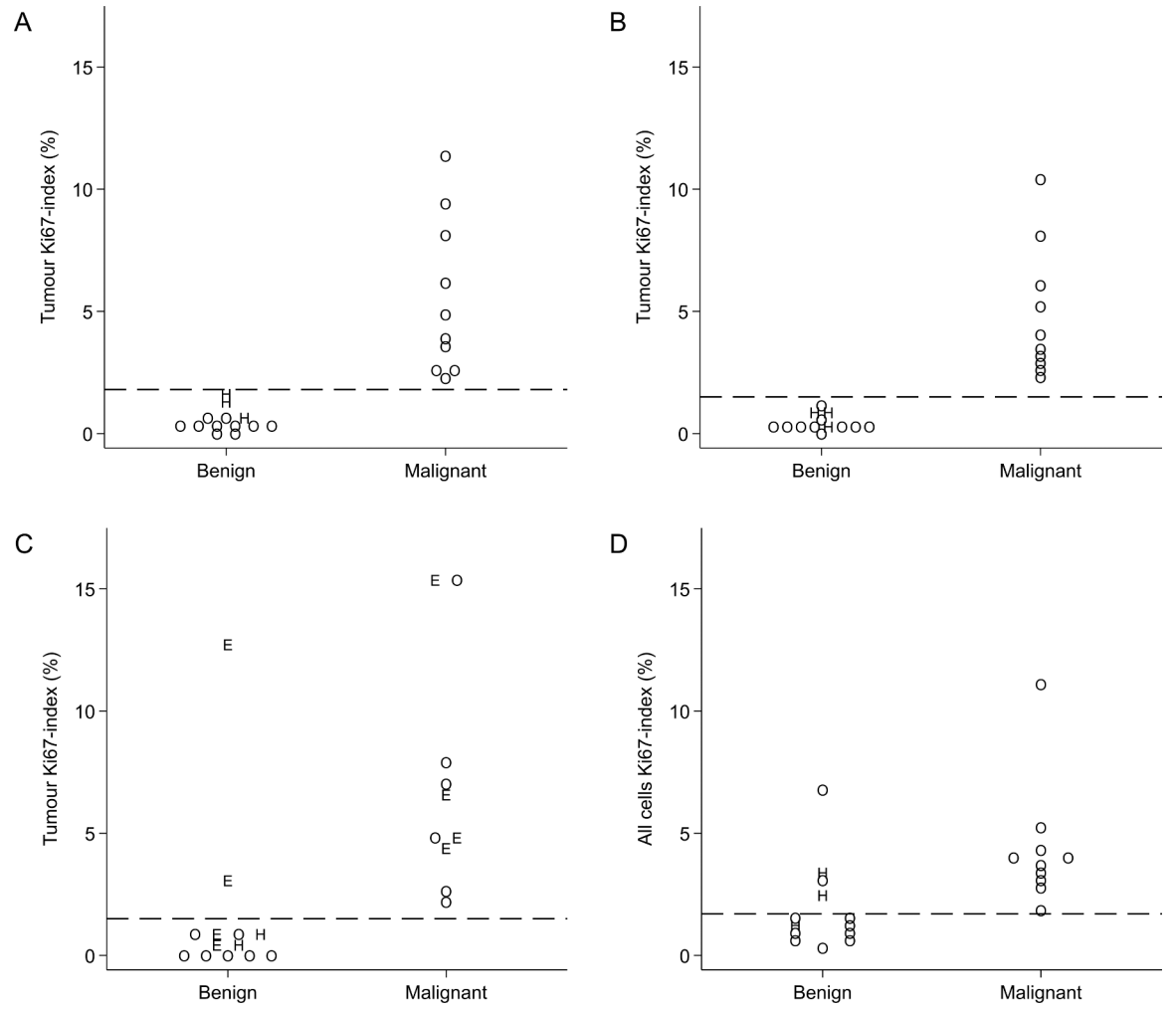

Fig. 2. Ki67-index in benign and malignant melanocytic lesions measured using double nuclear staining with three different methods: A) Multiplex immunofluorescence, Ki67-index threshold at 1.8% (n = 23), B) Multiplex chromogenic immunohistochemistry, Ki67-index threshold at 1.5% (n = 23), C) Multiplexed immunohistochemical consecutive staining on single slide (MICSSS), Ki67-index threshold at 1.5% (n = 15). D) Conventional chromogenic single Ki67 stain (Fast Red) without tumour-cell identification, Ki67-index threshold at 1.7% (n = 23). The digital image analysis quantified the Ki67-indexes in the total tumour ROI including the overlaying epidermis. Labels: O= included lesions, H= included halo nevi, E = excluded lesions.

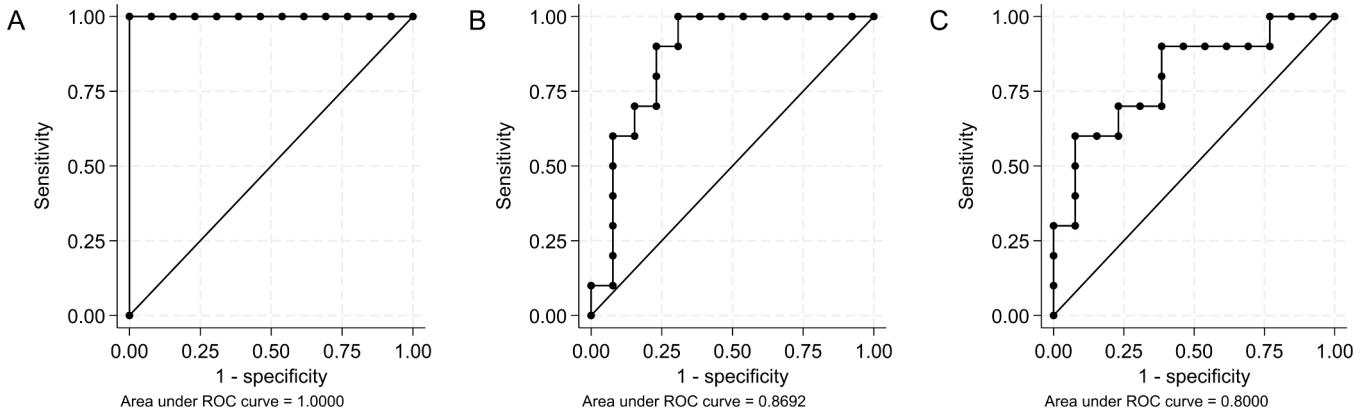

Fig. 3. ROC curves of automatically quantified Ki67-indexes with or without tumor-cell identification. ROC curves of Ki67-indexes (N = 23) measured as A) SOX10-verified Ki67-index: automated quantification of Ki67/SOX10 double nuclear staining by the mIHC method, B) 'Unverified' Ki67-index: automated quantification of all Ki67 positive nuclei out of all nuclei, and C) 'Unverified' Ki67 area index: automated quantification of all Ki67 positive nuclei per area of the manually outlined total tumour ROI including overlaying epidermis to mimic the clinical 'eyeballing' method. B and C are based on the Ki67 AP mono stain from the method multiplex immunohistochemical consecutive staining on single slide (MICSSS).

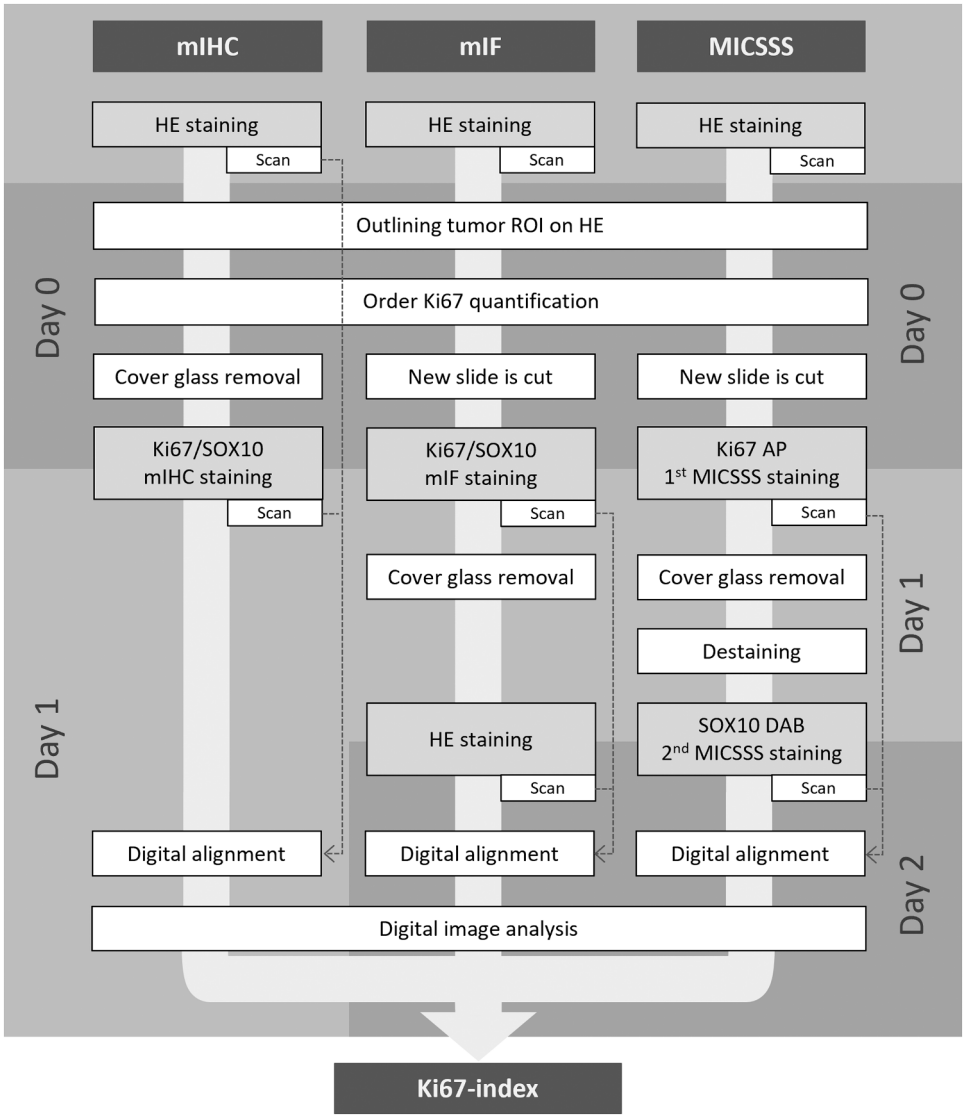

Fig. 4. Overview of workflows of double nuclear staining in a diagnostic setting at a digitalized pathology department. All workflows start with the obligatory initial hematoxylin and eosin (HE) stain. A Ki67 double nuclear stain is then performed using one of the three different methods: multiplex chromogenic immunohistochemistry (mIHC), multiplex immunofluorescence (mIF), and multiplexed immunohistochemical consecutive staining on single slide (MICSSS), followed by automated quantification of the Ki67 index by digital image analysis. In a digitalised department, the workflow of the mIHC method does not require more hands-on time by lab technicians, than the routine Ki67 workflow currently does: Based on the initial digital HE, the pathologist determined if additional stains are needed and selects the appropriate glass/block for these stains. In the current workflow in our lab, the technician would then find the block in the archive, cut a new section, put this on the staining machine and have the Ki67 mono stain ready for the pathologist the next day. In our proposed new workflow of the mIHC method, the technician would find the HE stained glass instead of the block, remove the coverglass by heat (a few seconds) and put this slide on the staining machine. The next day the mIHC Ki67/SOX10 double nuclear stain will be ready for scan and DIA and delivered to the pathologist.

magenta and turquoise yielding a blue colour shift as previously proposed by van der Loos et al. [31]. For mIHC, stable staining intensities are necessary. If the staining intensity varies, it becomes challenging to set an optimal fixed threshold, especially over time and between different laboratories. It is possible that future developments in DIA algorithms may include automated threshold adjustment or the use of artificial intelligence (AI) to address this issue. Furthermore, the general concern of variation in Ki67 stains across different laboratories [9,25] has led to the proposal of a new tool for Ki67 standardization, which may also apply for double nuclear staining [3,26].

MICSSS Ki67/SOX10 staining has the key advantage that it employs two routinely performed immunohistochemical stainings, separated by a de-staining and scanning step [1,23]. Most pathology departments equipped with a scanner can perform the procedure as it uses routine chromogens like Fast Red and DAB, in contrast to mIF and mIHC that are currently limited to research purposes. Moreover, the performance of separate staining and scanning steps in MICSSS ensures a clear differentiation between the two markers. General drawbacks of MICSSS include prolonged processing time by adding a day to the workflow [21, 30] and the inability to access the result manually under a microscope [21]. Furthermore, this method implicates several technical steps, that are susceptible to errors as 1) tissue artefacts coursed by cover glass removal, 2) inaccurate digital alignment, and 3) incomplete de-staining. In our study, tissue artefacts were minimised by careful handling and successfully digital alignment was achieved. Unfortunately, the issue of incomplete de-staining significantly affected our results. Despite making multiple attempts at protocol optimization, we could not completely remove the Fast Red chromogen in almost one-third of our cases. Previous studies have reported successful de-staining using AEC red [1,12], but our laboratory's Ventana platform is not compatible with AEC.

Given its alcohol solubility like AEC [1], the current de-staining issue with Fast Red is a puzzling problem. In fact, our DIA protocol could operate on slides, where some Fast Red staining remained, but heavily Fast Red stained nuclei posed a challenge that led to errors in the Ki67-indexes. As a result, we had to exclude approximately one-third of the specimens due to failed de-staining.

It is widely acknowledged that the Ki67-index is elevated in malignant melanocytic lesions compared with benign nevi [7]. By utilising the SOX10/Ki67 double nuclear stain for automated Ki67-quantification, we could, in all three methods, define a Ki67-index cut off that completely distinguished benign from malignant lesions, with an AUC of 1.0. The lesions were divided by Ki67-index cut-off points at 1.5% (mIHC and MICSSS) and 1.8% (mIF). This resembles the cut-off points of 1.6% and 1.8% from previous studies of automated quantification of Ki67 in melanocytic lesions [17,18]. Studies with manual interpretation of the Ki67-index have found similarly low levels in benign nevi, but generally higher Ki67-indexes in melanomas [20]. This may be because of inclusion of thicker lesions compared to the present study, and overestimation by counting infiltrating proliferative cells. The low Ki67 index thresholds seen in studies using digital quantification cannot be directly transferred to manual assessment in routine pathology. However, if DIA becomes widely used as a tool for Ki67 assessment, it will provide standardised measures and high reproducibility that will ensure comparable measures between individual pathologists and pathology departments.

It has been proposed that the Ki67-index of dermal compartment has the best discriminating power [5]. However, distinguishing the dermal from the epidermal compartment did not enhance the performance in the present study, which is in line with findings of Nielsen et al. [19] and Li et al. [15]. Our findings showed that limiting the image analysis to an outlined tumour area including overlaying epidermis results in better performance compared to analysing the whole slide. This could be attributed to errors occurring form artefacts as autofluorescent erythrocytes in subcutis (mIF) or red tush markings on the resection margin (MICSSS).

In the present study, we showed that the use of Ki67/SOX10 double nuclear stain enhanced the performance of the Ki67-index compared to Ki67 alone. This underlines that precise tumour-cell identification is essential for the diagnostic performance of automated Ki67-quantification. Precise tumour-cell identification seems to be especially important in inflamed lesions. The double nuclear stain combining a target biomarker with a tumour-cell marker can provide an ideal platform for quantitative digital image analysis in the future. This approach can be useful for many other tumour types that require precise tumour cell identification.

The ongoing digitalisation in pathology enables the use of DIA for diagnostic purposes. Pathology departments that have undergone digitalisation will be able to implement the workflows proposed in this study. Some of the proposed methods require extra manual work of laboratory technicians, but the workflow of the mIHC method has the same amount of hands-on time as the standard Ki67 mono-staining. In the mIF and mIHC workflows, the resulting DIA annotations are visualised on the combined multiplex and HE digital images, enabling the pathologists to visualize both the HE morphology and IHC marker positivity for each single cell (Fig. 1), and use the combined visual result in their final diagnostic assessment. Furthermore, the pathologists can validate the results of the DIA quantifications. The mIHC method can also be visualised in a traditional light microscope and used for manual Ki67 quantification and thereby be used in laboratories without access to DIA, for example, in small throughput laboratories.

5. Conclusion

In this proof-of-concept study, we optimised three immunohistochemical methods for automated quantification of Ki67/SOX10 double nuclear stain and tested their discriminative ability on a small cohort of melanocytic lesions. Our results indicated that the Ki67/SOX10 double nuclear stain improves the diagnostic precision of Ki67 interpretation. However, the results could benefit from validation on a lager study cohort. Of the three methods, the mIHC seems to be more suitable for everyday workflow. The study illustrates the potential of the Ki67/SOX10 double nuclear stain as a valuable diagnostic aid for melanocytic lesions.

Funding

This work was supported by Harboefonden, Denmark, Toyota-Fonden, Denmark, Dagmar Marshalls Fond, Denmark, and Health Research Foundation of Central Denmark Region, Denmark, (grant ID: A3139).

CRediT authorship contribution statement

Steiniche Torben: Writing – review & editing, Validation, Supervision, Methodology, Conceptualization. **Lade-Keller Johanne:** Writing – review & editing, Supervision. **Wandler Anne:** Writing – review & editing, Supervision. **Georgsen Jeanette Bæhr:** Writing – review & editing, Methodology, Investigation. **Christensen Kristina Bang:** Writing – review & editing, Methodology, Investigation. **Nielsen Patricia Switten:** Writing – review & editing, Supervision, Software, Methodology, Funding acquisition. **Brogård Mette Bak:** Writing – original draft, Visualization, Software, Project administration, Methodology, Investigation, Funding acquisition, Formal analysis, Conceptualization.

Declaration of Generative AI and AI-assisted technologies in the writing process

During the preparation of this work the authors used *ProWritingAid Anywhere for Windows -Grammarly for Your Desktop* (International House, 36–38 Cornhill, London EC3V 3NG, United Kingdom) in order to review the formulation of a few single sentences during the review and editing process. After using this tool/service, the authors reviewed and edited the content as needed and takes full responsibility for the content of the publication.

Declaration of Competing Interest

The authors declare the following financial interests/personal relationships which may be considered as potential competing interests: Mette Bak Brogaard reports financial support was provided by Harboe Foundation. Patricia Switten Nielsen reports financial support was provided by Toyota-Fonden, Denmark. Patricia Switten Nielsen reports financial support was provided by Dagmar Marshall Fund. Patricia Switten Nielsen reports financial support was provided by Health Research Foundation of Central Denmark Region. If there are other authors, they declare that they have no known competing financial interests or personal relationships that could have appeared to influence the work reported in this paper.

Appendix A. Supporting information

Supplementary data associated with this article can be found in the online version at doi:10.1016/j.prp.2024.155177.

References

[1] G. Akturk, R. Sweeney, R. Remark, M. Merad, S. Gnjatic, Multiplexed immunohistochemical consecutive staining on single slide (MICSSS): multiplexed chromogenic IHC assay for high-dimensional tissue analysis, Methods Mol. Biol. 2055 (2020) 497–519.

[2] C.C. Anyaegbu, T.F. Lee-Pullen, T.J. Miller, T.N. Abel, C.F. Platell, M.J. McCoy, Optimisation of multiplex immunofluorescence for a non-spectral fluorescence scanning system, J. Immunol. Methods 472 (2019) 25–34.
[3] T.N. Aung, B. Acs, J. Warrell, Y. Bai, P. Gaule, S. Martinez-Morilla, I. Vathiotis, S. Shafi, M. Moutafi, M. Gerstein, B. Freiberg, R. Fulton, D.L. Rimm, A new tool for technical standardization of the Ki67 immunohistochemical assay, Mod. Pathol. 34 (2021) 1261–1270.
[4] R.L. Barnhill, D.E. Elder, M.W. Piepkorn, S.R. Knezevich, L.M. Reisch, M.M. Eguchi, B.C. Bastian, W. Blokx, M. Bosenberg, K.J. Busam, R. Carr, A. Cochran, M.G. Cook, L.M. Duncan, R. Elenitsas, A. de la Fouchardiere, P. Gerami, I. Johansson, J. Ko, G. Landman, A.J. Lazar, L. Lowe, D. Massi, J. Messina, D. Mihic-Probst, D. C. Parker, B. Schmidt, C.R. Shea, R.A. Scolyer, M. Tetzlaff, X. Xu, I. Yeh, A. Zembowicz, J.G. Elmore, Revision of the melanocytic pathology assessment tool and hierarchy for diagnosis classification schema for melanocytic lesions: a consensus statement, JAMA Netw. Open 6 (2023) e2250613.
[5] R. Bergman, L. Malkin, E. Sabo, H. Kerner, MIB-1 monoclonal antibody to determine proliferative activity of Ki-67 antigen as an adjunct to the histopathologic differential diagnosis of Spitz nevi, J. Am. Acad. Dermatol. 44 (2001) 500–504.
[6] T. Chen, C. Srinivas, Group sparsity model for stain unmixing in brightfield multiplex immunohistochemistry images, Comput. Med Imaging Graph 46 (Pt 1) (2015) 30–39.
[7] L.E. Davis, S.C. Shalin, A.J. Tackett, Current state of melanoma diagnosis and treatment, Cancer Biol. Ther. 20 (2019) 1366–1379.
[8] J.G. Elmore, R.L. Barnhill, D.E. Elder, G.M. Longton, M.S. Pepe, L.M. Reisch, P. A. Carney, L.J. Titus, H.D. Nelson, T. Onega, A.N.A. Tosteson, M.A. Weinstock, S. R. Knezevich, M.W. Piepkorn, Pathologists' diagnosis of invasive melanoma and melanocytic proliferations: observer accuracy and reproducibility study, BMJ 357 (2017) j2813.
[9] R. Fulton, Getting a Grip on Ki-67, Appl. Immunohistochem. Mol. Morphol. 29 (2021) 83–85.
[10] M.J. Gerdes, C.J. Sevinsky, A. Sood, S. Adak, M.O. Bello, A. Bordwell, A. Can, A. Corwin, S. Dinn, R.J. Filkins, D. Hollman, V. Kamath, S. Kaanumalle, K. Kenny, M. Larsen, M. Lazare, Q. Li, C. Lowes, C.C. McCulloch, E. McDonough, M. C. Montalto, Z. Pang, J. Rittscher, A. Santamaria-Pang, B.D. Sarachan, M.L. Seel, A. Seppo, K. Shaikh, Y. Sui, J. Zhang, F. Ginty, Highly multiplexed single-cell analysis of formalin-fixed, paraffin-embedded cancer tissue, Proc. Natl. Acad. Sci. USA 110 (2013) 11982–11987.
[11] J.E. Gershenwald, R.A. Scolyer, Melanoma staging: american joint committee on cancer (AJCC) 8th edition and beyond, Ann. Surg. Oncol. 25 (2018) 2105–2110.
[12] G. Glass, J.A. Papin, J.W. Mandell, SIMPLE: a sequential immunoperoxidase labeling and erasing method, J. Histochem Cytochem 57 (2009) 899–905.
[13] D. Ivan, V.G. Prieto, Use of immunohistochemistry in the diagnosis of melanocytic lesions: applications and pitfalls, Future Oncol. 6 (2010) 1163–1175.
[14] H. Lara, Z. Li, E. Abels, F. Aeffner, M.M. Bui, E.A. ElGabry, C. Kozlowski, M. C. Montalto, A.V. Parwani, M.D. Zarella, D. Bowman, D. Rimm, L. Pantanowitz, Quantitative image analysis for tissue biomarker use: a white paper from the digital pathology association, Appl. Immunohistochem. Mol. Morphol. 29 (2021) 479–493.
[15] L.X. Li, K.A. Crotty, S.W. McCarthy, A.A. Palmer, J.J. Kril, A zonal comparison of MIB1-Ki67 immunoreactivity in benign and malignant melanocytic lesions, Am. J. Derm. 22 (2000) 489–495.
[16] M.K.K. Niazi, A.V. Parwani, M.N. Gurcan, Digital pathology and artificial intelligence, Lancet Oncol. 20 (2019) e253–e261.
[17] P.S. Nielsen, R. Riber-Hansen, J. Raundahl, T. Steiniche, Automated quantification of MART1-verified Ki67 indices by digital image analysis in melanocytic lesions, Arch. Pathol. Lab Med 136 (2012) 627–634.
[18] P.S. Nielsen, R. Riber-Hansen, T. Steiniche, Immunohistochemical double stains against Ki67/MART1 and HMB45/MITF: promising diagnostic tools in melanocytic lesions, Am. J. Derm. 33 (2011) 361–370.
[19] P.S. Nielsen, E. Spaun, R. Riber-Hansen, T. Steiniche, Automated quantification of MART1-verified Ki-67 indices: useful diagnostic aid in melanocytic lesions, Hum. Pathol. 45 (2014) 1153–1161.
[20] S.J. Ohsie, G.P. Sarantopoulos, A.J. Cochran, S.W. Binder, Immunohistochemical characteristics of melanoma, J. Cutan. Pathol. 35 (2008) 433–444.
[21] E.R. Parra, M. Ilie, I.I. Wistuba, P. Hofman, Quantitative multiplexed imaging technologies for single-cell analysis to assess predictive markers for immunotherapy in thoracic immuno-oncology: promises and challenges, Br. J. Cancer (2023).
[22] M.D. Reid, P. Bagci, N. Ohike, B. Saka, I. Erbarut Seven, N. Dursun, S. Balci, H. Gucer, K.T. Jang, T. Tajiri, O. Basturk, S.Y. Kong, M. Goodman, G. Akkas, V. Adsay, Calculation of the Ki67 index in pancreatic neuroendocrine tumors: a comparative analysis of four counting methodologies, Mod. Pathol. 28 (2015) 686–694.
[23] R. Remark, T. Merghoub, N. Grabe, G. Litjens, D. Damotte, J.D. Wolchok, M. Merad, S. Gnjatic, In-depth tissue profiling using multiplexed immunohistochemical consecutive staining on single slide, Sci. Immunol. 1 (2016) aaf6925.
[24] D. Robertson, K. Savage, J.S. Reis-Filho, C.M. Isacke, Multiple immunofluorescence labelling of formalin-fixed paraffin-embedded (FFPE) tissue, BMC Cell Biol. 9 (2008) 13.
[25] R. Roge, S. Nielsen, R. Riber-Hansen, M. Vyberg, Impact of primary antibody clone, format, and stainer platform on ki67 proliferation indices in breast carcinomas, Appl. Immunohistochem. Mol. Morphol. 27 (2019) 732–739.
[26] R. Roge, S. Nielsen, R. Riber-Hansen, M. Vyberg, Image Analyses Assessed Cell Lines as Potential Performance Controls of Ki-67 Immunostained Slides, Appl. Immunohistochem. Mol. Morphol. 29 (2021) 95–98.
[27] A. Saleem, S. Narala, S.S. Raghavan, Immunohistochemistry in melanocytic lesions: updates with a practical review for pathologists, Semin Diagn. Pathol. 39 (2022) 239–247.
[28] W. Sheng, C. Zhang, T.M. Mohiuddin, M. Al-Rawe, F. Zeppernick, F.H. Falcone, I. Meinhold-Heerlein, A.F. Hussain, Multiplex immunofluorescence: a powerful tool in cancer immunotherapy, Int J. Mol. Sci. 24 (2023).
[29] D. Tacha, W. Qi, S. Ra, R. Bremer, C. Yu, J. Chu, L. Hoang, B. Robbins, A newly developed mouse monoclonal SOX10 antibody is a highly sensitive and specific marker for malignant melanoma, including spindle cell and desmoplastic melanomas, Arch. Pathol. Lab Med 139 (2015) 530–536.
[30] J.M. Taube, G. Akturk, M. Angelo, E.L. Engle, S. Gnjatic, S. Greenbaum, N. F. Greenwald, C.V. Hedvat, T.J. Hollmann, J. Juco, E.R. Parra, M.C. Rebelatto, D. L. Rimm, J. Rodriguez-Canales, K.A. Schalper, E.C. Stack, C.S. Ferreira, K. Korski, A. Lako, S.J. Rodig, E. Schenck, K.E. Steele, M.J. Surace, M.T. Tetzlaff, K. von Loga, I.I. Wistuba, C.B. Bifulco, F. Society for Immunotherapy of Cancer Pathology Task, The Society for Immunotherapy of Cancer statement on best practices for multiplex immunohistochemistry (IHC) and immunofluorescence (IF) staining and validation, J. Immunother. Cancer 8 (2020).
[31] C.M. van der Loos, Multiple immunoenzyme staining: methods and visualizations for the observation with spectral imaging, J. Histochem Cytochem 56 (2008) 313–328.
[32] A. Wandler, E. Spaun, T. Steiniche, P.S. Nielsen, Automated quantification of Ki67/MART1 stains may prevent false-negative melanoma diagnoses, J. Cutan. Pathol. 43 (2016) 956–962.
[33] K.A. Wharton Jr., D. Wood, M. Manesse, K.H. Maclean, F. Leiss, A. Zuraw, Tissue multiplex analyte detection in anatomic pathology - pathways to clinical implementation, Front Mol. Biosci. 8 (2021) 672531.
[34] W. Zhang, A. Hubbard, T. Jones, A. Racolta, S. Bhaumik, N. Cummins, L. Zhang, K. Garsha, F. Ventura, M.R. Lefever, Z. Lu, J.K. Hurley, W.A. Day, L. Pestic-Dragovich, L.E. Morrison, L. Tang, Fully automated 5-plex fluorescent immunohistochemistry with tyramide signal amplification and same species antibodies, Lab Invest 97 (2017) 873–885.